

# Effects of autotransformer's stabilizing winding on current-voltage conditions during unsymmetrical faults

Tomislav Pavicic, Bozidar Filipovic-Grcic, Dalibor Filipovic-Grcic, Bruno Jurisic

**Abstract** - In this paper, model of three-phase autotransformer with stabilizing winding is developed in EMTP for short-circuit studies. Currents and voltages are determined inside transformer windings during unsymmetrical faults in the power system. Influence of delta connected stabilizing winding on current-voltage conditions is analysed. Results obtained by EMTP model are compared with the inductance matrix model of autotransformer developed in Matlab, consisting of winding self-inductances and corresponding mutual inductances between windings.

**Keywords:** autotransformer, stabilizing winding, EMTP model, short-circuit, matrix inductance model.

## I. INTRODUCTION

An autotransformer is a special type of power transformer in which the energy between the primary and secondary side is transferred both electromagnetically and galvanically. Autotransformer has one parallel winding which is shared between primary and secondary side. That's the main reason why autotransformers are cheaper and more used in power systems. Besides parallel winding, autotransformer also has a series winding, and may have a delta connected stabilizing winding. During the lifetime autotransformer is exposed to numerous dielectric, thermal and mechanical stresses caused by overvoltages and short-circuits in the power transmission network. If single phase to ground short-circuit occurs in the network with power transformers having isolated neutral points, temporary overvoltages will appear in healthy phases [1]. However, the common industrial practice is to solidly connect the autotransformer neutral to the substation earthing system. Neutral point can be isolated or grounded over impedance to limit excessive values of short-circuit currents. This approach is used mainly in strong meshed networks or nearby large power plants, where the single-phase fault current could exceed the three-phase fault current [2]. In this paper all different possibilities of neutral grounding are considered, from

isolated to solidly grounded. In the cases when neutral point is directly grounded or grounded over low impedance, no significant overvoltages are generally expected on healthy phases when using autotransformer without stabilizing winding.

Delta winding presence strongly affects autotransformer zero sequence impedance and it permits the flow of third harmonic current. That is one of the main reasons why stabilizing winding is used for reduction of voltage harmonics and unbalances in the network [3]. Stabilizing winding usually has the lowest rated voltage. Historically, transformer's tertiary stabilizing windings were designed to be approximately third of the rated power, but stabilizing windings shall be designed to withstand thermal stress caused by circulating currents resulting from continuous and temporary load or voltage unbalance on the main windings [4],[5]. Tertiary winding should also withstand mechanical stress caused by short-circuit currents. Faults can occur at tertiary winding leading to serious transformer failures. Tertiary winding is used for supplying energy to connected loads while stabilizing winding is not used for this purpose but only for stabilizing the neutral point of the fundamental frequency voltages, to eliminate excessive third harmonic, and to provide an internally closed circuit for zero sequence currents. In the case of stabilizing winding, one corner of delta is grounded and for this purpose only two connections are available from outside of the transformer tank. This eliminates possibility of fault occurrence when using stabilizing winding, compared to tertiary winding [3]. Drawback of using power transformers with delta-closed stabilizing windings is that in some cases short-circuit currents will be higher and this consequently increases electrodynamic (mechanical) stress [6].

References [7]-[9] describe the autotransformer models used for steady state analysis such as short-circuit or load flow calculation, while in [10] autotransformer model is used during analysis of transient recovery voltage. However, specific autotransformer terminal faults and influence of stabilizing winding during such faults on current-voltage conditions are not broadly investigated in the literature.

Autotransformer model presented in [11] is used for simulation of unsymmetrical faults. This model is based on autotransformer inductance matrix and it was successfully verified by comparing the results with ones obtained by symmetrical components, which is a well-known method used for short-circuit analysis. In this paper, autotransformer model with delta winding is developed in EMTP software which performs the calculation in the time domain. Model is validated by comparing simulation results with the ones obtained by

---

T. Pavicic is with the Končar Power Transformers, Josipa Mokrovića 6, 10090 Zagreb, Croatia (email: tomlav.pavicic@siemens-energy.com).

B. Filipovic-Grcic is with the University of Zagreb, Faculty of Electrical Engineering and Computing, Unska 3, 10000 Zagreb, Croatia (email: bozidar.filipovic-grcic@fer.hr).

D. Filipovic-Grcic and B. Jurisic are with the Končar – Electrical Engineering Institute, 10000 Zagreb, Croatia (email: dfilipovic@koncar-institut.hr; bjurisic@koncar-institut.hr).

inductance matrix model developed in Matlab (*m-file*). Finally, the influence of the stabilization winding on the current-voltage conditions during a short-circuit is analysed. **Developed autotransformer model can be used for short-circuit calculations or for analysis of relay protection operation [12].**

## II. INDUCTANCE MATRIX MODEL

Autotransformer model [11] is based on inductance matrix which is formed from winding self-inductances and mutual inductances between windings. Only inductive component of autotransformer winding impedance is considered in the model since resistance component of the impedance can be neglected compared to the inductance component. This assumption is physically justified, and it gives slightly increased short-circuit currents, which means that calculation is on the safe side.

Parameters used for autotransformer model are obtained from manufacturer data based on factory measurements. First, open-circuit test data are used to determine the self-inductance  $L_1$  of series and parallel winding (1):

$$L_1 = \frac{U_{r1}^2}{\omega \cdot I_0 \cdot S_r} \cdot 100 \quad (1)$$

where  $I_0$  represents magnetizing current expressed in percent with regard to the rated current,  $U_{r1}$  rated voltage of high voltage winding,  $S_r$  rated power of transformer and  $\omega$  angular frequency.

Self-inductances  $L_s$  of the series winding,  $L_p$  of the parallel winding and  $L_3$  of the stabilizing winding are determined from (2)-(4):

$$L_s = L_1 \cdot \left( \frac{U_{r1} - U_{r2}}{U_{r1}} \right)^2 \quad (2)$$

$$L_p = L_1 \cdot \left( \frac{U_{r2}}{U_{r1}} \right)^2 \quad (3)$$

$$L_3 = \frac{U_{r3}^2}{\omega \cdot I_0 \cdot S_r} \cdot 100 \cdot 3 \quad (4)$$

where  $U_{r2}$  represents rated voltage of the parallel winding and  $U_{r3}$  rated voltage of stabilizing winding.

Mutual inductance between parallel and series winding  $M_{sp}$  can be obtained from the circuit shown in Fig. 1. Voltage is increased at high-voltage side until rated current  $I_{r1}$  is obtained, while low-voltage winding is short-circuited.

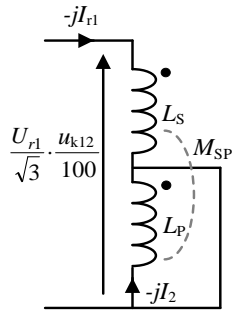


Fig. 1. Test circuit – estimation of  $M_{sp}$

Direction of current through parallel winding  $I_2$  is opposite to  $I_{r1}$ . The Eqs. (5) and (6) are extracted from the circuit shown in Fig. 1.

$$\frac{U_{r1}}{\sqrt{3}} \cdot \frac{u_{k12}}{100} = I_{r1} \omega (L_s + M_{sp}) - I_2 \omega (L_p + M_{sp}) \quad (5)$$

$$I_2 = I_{r1} \frac{M_{sp}}{L_p} \quad (6)$$

$u_{k12}$  represents the rated short-circuit voltage with regard to apparent rated power  $S_{r12}$  between high-voltage and low-voltage winding.  $U_{r1}$  is the rated voltage of high-voltage winding. Mutual inductance  $M_{sp}$  can be determined from following expression (7).

$$M_{sp} = \sqrt{\left( I_{r1} \omega L_s - \frac{U_{r1}}{\sqrt{3}} \cdot \frac{u_{k12}}{100} \right) \cdot \frac{L_p}{I_{r1} \omega}} \quad (7)$$

$M_{p3}$  represents mutual inductance between parallel and stabilizing winding (10). This mutual inductance can be determined from the circuit shown in Fig. 2. Voltage is applied on low-voltage winding, with short-circuited stabilizing winding. The expression (8) and (9) are derived from the circuit shown in Fig. 2.

$$\frac{U_{r2}}{\sqrt{3}} \cdot \frac{u_{k23}}{100} = I_{r2} \omega L_p - I_3 \omega M_{p3} \quad (8)$$

$$I_3 = I_{r2} \frac{M_{p3}}{L_3} \quad (9)$$

$$M_{p3} = \sqrt{\left( I_{r2} \omega L_p - \frac{U_{r2}}{\sqrt{3}} \cdot \frac{u_{k23}}{100} \right) \cdot \frac{L_3}{I_{r2} \omega}} \quad (10)$$

$u_{k23}$  represents the rated short-circuit voltage with regard to apparent rated power  $S_{r23}$  between low-voltage and stabilizing winding.  $U_{r2}$  represents rated voltage of low-voltage winding.

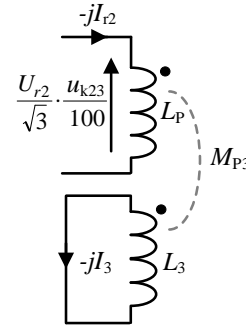


Fig. 2. Test circuit – estimation of  $M_{p3}$

$M_{s3}$  represents mutual inductance between series and stabilizing winding (13). This mutual inductance can be determined from the circuit shown in Fig. 3.

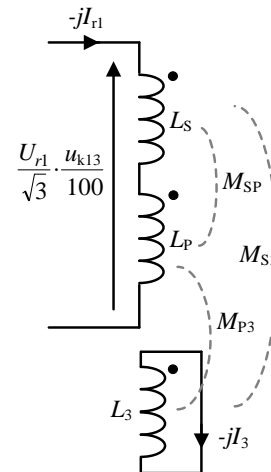


Fig. 3. Test circuit – estimation of  $M_{s3}$

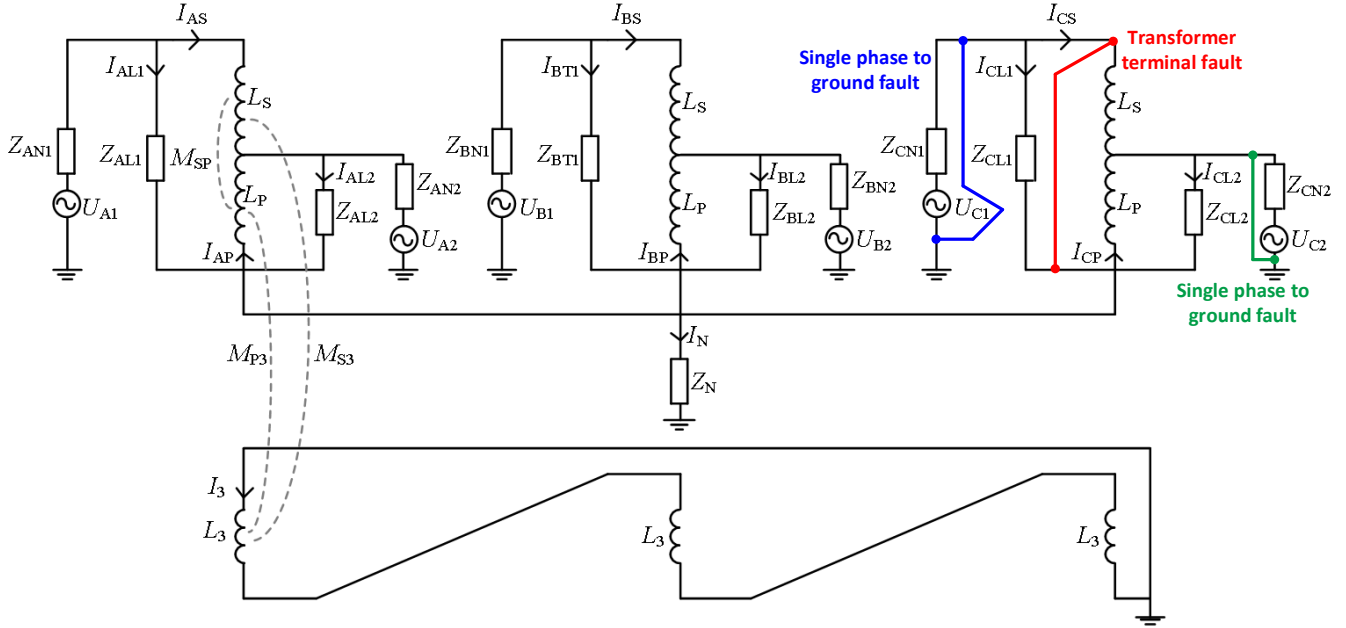


Fig. 4. Three-phase autotransformer model (analysed faults: red - transformer terminal fault in phase C between HV winding and transformer's neutral grounding point; blue - single phase to ground fault in phase C at HV side; green - single phase to ground fault in phase C at LV side)

$$\begin{bmatrix} U_{A1} \\ U_{B1} \\ U_{C1} \\ U_{A2} \\ U_{B2} \\ U_{C2} \\ U_{A1} \\ U_{B1} \\ U_{C1} \\ U_{A2} \\ U_{B2} \\ U_{C2} \\ 0 \\ 0 \\ 0 \end{bmatrix} = \begin{bmatrix} Z_{AN1} & 0 & 0 & 0 & 0 & 0 & Z_{AN1} + X_S + X_{SP} & 0 & 0 & -(X_P + X_{SP}) & 0 & 0 & Z_N & X_{S3} + X_{P3} \\ 0 & Z_{BN1} & 0 & 0 & 0 & 0 & 0 & Z_{BN1} + X_S + X_{SP} & 0 & 0 & -(X_P + X_{SP}) & 0 & Z_N & X_{S3} + X_{P3} \\ 0 & 0 & Z_{CN1} & 0 & 0 & 0 & 0 & 0 & Z_{CN1} + X_S + X_{SP} & 0 & 0 & -(X_P + X_{SP}) & Z_N & X_{S3} + X_{P3} \\ 0 & 0 & 0 & Z_{AN2} & 0 & 0 & X_{SP} - Z_{AN2} & 0 & 0 & 0 & -(Z_{AN2} + X_P) & 0 & Z_N & X_{P3} \\ 0 & 0 & 0 & 0 & Z_{BN2} & 0 & 0 & X_{SP} - Z_{BN2} & 0 & 0 & 0 & -(Z_{BN2} + X_P) & Z_N & X_{P3} \\ 0 & 0 & 0 & 0 & 0 & Z_{CN2} & 0 & 0 & X_{SP} - Z_{CN2} & 0 & 0 & -(Z_{CN2} + X_P) & Z_N & X_{P3} \\ Z_{AN1} + Z_{AL1} & 0 & 0 & 0 & 0 & 0 & Z_{AN1} & 0 & 0 & 0 & 0 & 0 & Z_N & 0 \\ 0 & Z_{BN1} + Z_{BL1} & 0 & 0 & 0 & 0 & 0 & Z_{BN1} & 0 & 0 & 0 & 0 & Z_N & 0 \\ 0 & 0 & Z_{CN1} + Z_{CL1} & 0 & 0 & 0 & 0 & 0 & Z_{CN1} & 0 & 0 & 0 & Z_N & 0 \\ 0 & 0 & 0 & Z_{AN2} + Z_{AL2} & 0 & 0 & -Z_{AN2} & 0 & 0 & -Z_{AN2} & 0 & 0 & Z_N & 0 \\ 0 & 0 & 0 & 0 & Z_{BN2} + Z_{BL2} & 0 & -Z_{BN2} & 0 & 0 & -Z_{BN2} & 0 & 0 & Z_N & 0 \\ 0 & 0 & 0 & 0 & 0 & Z_{CN2} + Z_{CL2} & -Z_{CN2} & 0 & 0 & -Z_{CN2} & 0 & 0 & Z_N & 0 \\ 0 & 0 & 0 & 0 & 0 & 0 & X_{S3} & X_{S3} & -X_{P3} & -X_{P3} & -X_{P3} & -X_{P3} & 0 & 3X_{S3} \\ -1 & -1 & -1 & -1 & -1 & -1 & 0 & 0 & 0 & 1 & 1 & 1 & 1 & 0 \end{bmatrix} \times \begin{bmatrix} I_{BL1} \\ I_{AS} \\ I_{CS} \\ I_{CL2} \\ I_{BP} \\ I_{CP} \\ I_N \\ I_3 \end{bmatrix} \quad (22)$$

Voltage is applied on high-voltage side, with short-circuited stabilizing winding. Expression (11) and (12) are formed from the circuit shown in Fig. 3.

$$\frac{U_{r1}}{\sqrt{3}} \cdot \frac{u_{k13}}{100} = I_{r1} \omega (L_S + L_P + 2M_{SP}) - I_3 \omega (M_{S3} + M_{P3}) \quad (11)$$

$$I_3 = I_{r1} \frac{M_{P3} + M_{S3}}{L_3} \quad (12)$$

$u_{k13}$  represents the rated short-circuit voltage with regard to apparent rated power  $S_{r13}$  between high-voltage and stabilizing winding.

$$M_{S3} = \sqrt{L_3 (L_S + L_P + 2M_{SP}) - \frac{U_{r1}}{\sqrt{3}} \cdot \frac{u_{k13}}{100} \cdot \frac{L_3}{I_{r1} \omega}} - M_3 \quad (13)$$

Active networks from high-voltage and low-voltage side are modelled by impedances  $Z_{AN1}$  and  $Z_{AN2}$  placed behind voltage sources:

$$Z_{AN1} = j \frac{U_{r1}^2}{S_{SC1}} \quad (14)$$

$$Z_{AN2} = j \frac{U_{r2}^2}{S_{SC2}} \quad (15)$$

where  $S_{SC1}$  and  $S_{SC2}$  represent short-circuit powers of active networks on high-voltage and low-voltage side. Final three-phase autotransformer model is shown in Fig. 4. Short-circuit faults from high-voltage and low-voltage side are simulated by impedances  $Z_{AL1}$  and  $Z_{AL2}$ , while autotransformer ground impedance is represented by  $Z_N$ . From Fig. 4, expressions (16)

and (17) are derived for phase A at high-voltage side and expressions (18) and (19) are derived for phase A at low-voltage side. The same way expressions are derived for other two phases at high-voltage and low voltage side.

$$U_{A1} = (I_{AL1} + I_{AS}) \cdot Z_{AN1} + I_{AS} j \omega L_S - I_{AP} j \omega L_P + I_N Z_N - I_{AP} j \omega M_{SP} + I_{AS} j \omega M_{SP} + I_3 j \omega M_{S3} + I_3 j \omega M_{P3} \quad (16)$$

$$U_{A1} = (I_{AL1} + I_{AS}) \cdot Z_{AN1} + I_{AL1} Z_{AL1} + I_N Z_N \quad (17)$$

$$U_{A2} = (I_{AL2} - I_{AS} - I_{AP}) \cdot Z_{AN2} - I_{AP} j \omega L_P + I_N Z_N + I_{AS} j \omega M_{SP} + I_3 j \omega M_{P3} \quad (18)$$

$$U_{A2} = (I_{AL2} - I_{AS} - I_{AP}) \cdot Z_{AN2} + I_{AL2} Z_{AL2} + I_N Z_N \quad (19)$$

Expressions (20) and (21) are derived from Kirchhoff's current law:

$$(I_{AP} + I_{BP} + I_{CP}) \cdot j \omega M_{P3} = (I_{AS} + I_{BS} + I_{CS}) \cdot j \omega M_{S3} + 3I_3 j \omega L_3 \quad (20)$$

$$I_{AP} + I_{BP} + I_{CP} + I_N = I_{AL1} + I_{BL1} + I_{CL1} + I_{AL2} + I_{BL2} + I_{CL2} \quad (21)$$

Derived transformer equations can be written in the matrix form (22). Current vector  $\mathbf{I}$  can be determined from the following expression:

$$\mathbf{I} = \mathbf{Z}^{-1} \cdot \mathbf{U}. \quad (23)$$

### III. EMTP MODEL OF AUTOTRANSFORMER

The BCTRAN module in EMTP is used for autotransformer modelling based on data given in Table 1. BCTRAN module requires the entry of basic transformer data and produces an output in the form of  $[\mathbf{R}]$  and  $[\mathbf{L}]$  matrices. In BCTRAN module, parallel and series winding are modelled separately and therefore transformer data from Table 1 need to be adjusted.

TABLE I  
DATA USED FOR AUTOTRANSFORMER MODELLING

$U_{r1}$ (kV)	$U_{r2}$ (kV)	$U_{r3}$ (kV)
400	231	10.5
$u_{k12}$ (%)	$u_{k13}$ (%)	$u_{k23}$ (%)
11.63	13.92	10.66
$S_{r12}$ (MVA)	$S_{r13}$ (MVA)	$S_{r23}$ (MVA)
400	80	80

Rated phase voltages of series ( $U_s$ ), parallel ( $U_p$ ) and stabilizing ( $U_{r3}$ ) winding respectively are (Fig. 5):

$$U_s = \frac{U_{r1} - U_{r2}}{\sqrt{3}} = \frac{400 - 231}{\sqrt{3}} \text{ kV} = 97,57 \text{ kV} \quad (24)$$

$$U_p = \frac{U_{r2}}{\sqrt{3}} = \frac{231}{\sqrt{3}} \text{ kV} = 133,37 \text{ kV} \quad (25)$$

$$U_{r3} = 10,5 \text{ kV} \quad (26)$$

In addition to the rated voltages of transformer, for a proper determination of the  $[\mathbf{L}]$  matrix, it is necessary to enter the short-circuit impedances correctly. Data from Table I are given for short-circuit tests between: HV side and LV winding ( $u_{k12}$ ), HV side and stabilizing winding ( $u_{k13}$ ), and LV winding and stabilizing winding ( $u_{k23}$ ). In BCTRAN model it is assumed that short-circuit input impedance in the zero-sequence test is equal to the one in the positive-sequence test, which is valid for autotransformer (vector group YNa0d5) with five limb core and stabilizing winding. In case when inner geometry of transformer is known, zero-sequence impedance and inductance matrix can be calculated using finite element method (FEM). Due to the separate modelling of the series and parallel winding, it is necessary to determine the short-circuit impedances between windings: series-parallel ( $u_{ksp}$ ), series-stabilizing ( $u_{ks3}$ ) and parallel-stabilizing ( $u_{kp3}$ ), as shown in Fig. 5.

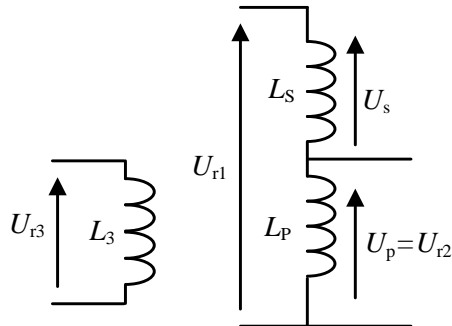


Fig. 5. Windings scheme in EMTP autotransformer model

Before applying expressions (27)-(29), it is necessary to recalculate short-circuit impedances at the same base power. Selected base power is 400 MVA. Open circuit test data

determine the values of inductance and resistance in magnetizing branch, but their values can be neglected in case of short-circuit studies.

$$u_{ksp} = u_{k12} \cdot \left( \frac{U_{r1}}{U_{r1} - U_{r2}} \right)^2 \quad (27)$$

$$u_{kp3} = u_{k23} \quad (28)$$

$$u_{ks3} = u_{k12} \cdot \frac{U_{r1} \cdot U_{r2}}{(U_{r1} - U_{r2})^2} + u_{k13} \cdot \frac{U_{r1}}{U_{r1} - U_{r2}} - u_{k23} \cdot \frac{U_{r2}}{U_{r1} - U_{r2}} \quad (29)$$

Equivalent scheme of EMTP model for simulation of faults is shown in Fig. 6. Simulations include single phase to ground fault at transformer terminals considering different neutral grounding impedances (fault is marked with red colour in Fig. 4).

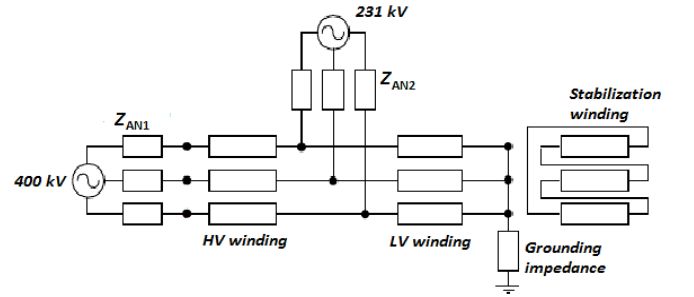


Fig. 6. Equivalent scheme of EMTP model

Three phase short-circuit powers from high-voltage and low-voltage side are equal to  $S_{scHV}=11.9$  GVA and  $S_{scLV}=3.43$  GVA, respectively. In all simulations voltage sources of active networks are directly grounded while transformer neutral grounding impedance is varied.

### IV. SIMULATION RESULTS AND COMPARISON BETWEEN MATRIX INDUCTANCE MODEL AND EMTP SIMULATIONS

Transformer terminal fault in phase C between HV winding and neutral point (marked with red colour in Fig. 4) is analysed considering different values of neutral grounding impedances. Calculation results are shown in Table II. Currents through transformer windings (series, parallel and stabilizing) are analysed and results are given both for EMTP model and inductance matrix model.  $I_{serC}$  is current through series winding and  $I_{parC}$  is current through parallel winding of the faulted phase C.  $I_{stab}$  is current through stabilizing winding. As shown in Table II, the percentage result differences  $\Delta_{max}$  between EMTP and inductance matrix model are almost negligible. Thereby, correctness of both developed models is confirmed, and EMTP model is further used in analysing the effects of stabilizing winding on current-voltage conditions.

Dependence of transformer currents with respect to the transformer neutral grounding impedance is shown in Fig. 7.  $I_{serA,B}$  is the current through series windings of healthy phases A and B while  $I_N$  represents the current through neutral grounding impedance. As expected, current through grounding impedance and current through faulted phase decrease with the increase of grounding impedance but at the same time the current through stabilizing winding increases. Such high

current stresses should be taken into consideration while designing the stabilizing winding particularly if the transformer neutral is grounded through high impedance or completely isolated.

TABLE II  
CURRENTS IN AUTOTRANSFORMER WINDINGS DURING TRANSFORMER  
TERMINAL FAULT IN PHASE C – COMPARISON BETWEEN EMT  
AUTOTRANSFORMER MODEL AND INDUCTANCE MATRIX MODEL

$R[\Omega] \setminus I[A]$		$I_{serC}$	$I_{parC}$	$I_{stab}$
$R = 0$	Inductance matrix model	2528.91	1633.32	2754.14
	EMTP (BCTRAN)	2530.05	1632.57	2755.75
$R = 10$	Inductance matrix model	1483.13	1618.15	16916.80
	EMTP (BCTRAN)	1483.93	1617.95	16916.50
$R = 100$	Inductance matrix model	186.11	1610.27	20734.89
	EMTP (BCTRAN)	186.47	1610.53	20733.96
$R = \infty$	Inductance matrix model	36.21	1610.14	20788.19
	EMTP (BCTRAN)	36.43	1610.32	20787.24
$\Delta_{max}[\%]$		0.603	0.046	0.058

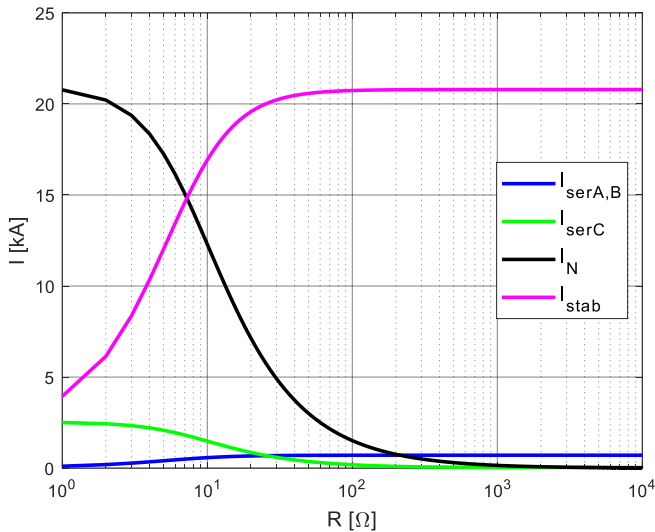


Fig. 7. Currents during transformer terminal fault with respect to the neutral grounding impedance

Influence of stabilizing winding on voltage conditions is shown in Fig. 8. Potential of neutral point follows half-circular path (marked by black dotted lines) which depends on ground impedance ranging from solidly grounded neutral ( $R=0$ ) to isolated neutral ( $R=\infty$ ). These calculations are performed in  $1 \Omega$  steps. Voltages in healthy phases increase with increasing grounding impedance. Delta connected stabilizing winding reduces zero-sequence impedance and, as consequence, voltages in the healthy phases will be reduced for autotransformers with stabilizing winding. Because of half-circular path of neutral point potential with respect to grounding impedance shown in Fig. 8, windings in healthy phases A and B experience different voltage stresses. Ratio of voltage in

healthy phases and their rated voltage with respect to grounding impedance is shown in Fig. 9.

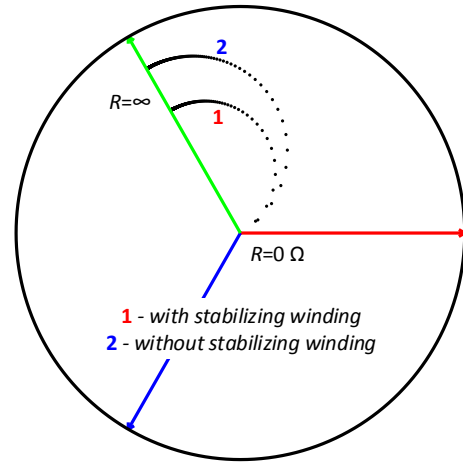


Fig. 8. Voltage potential of transformer neutral point in case of resistive grounding impedance (faulted phase C – green)

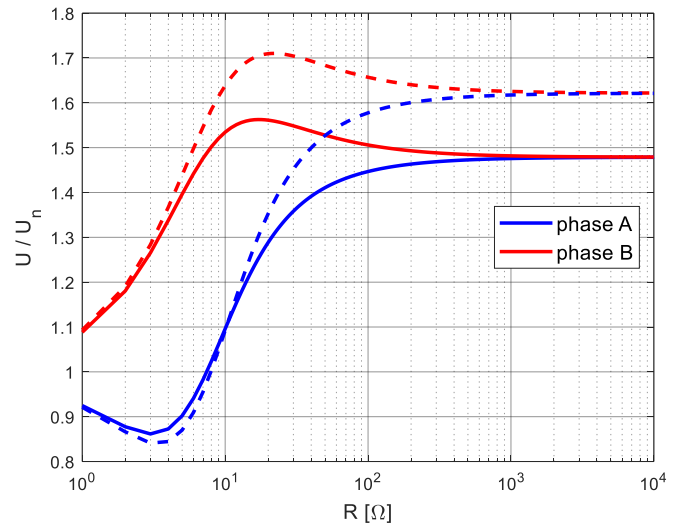


Fig. 9. Healthy phase voltages at transformer terminals with respect to the neutral grounding impedance (dashed lines represent the case without stabilizing winding and solid lines represent the case with stabilizing winding)

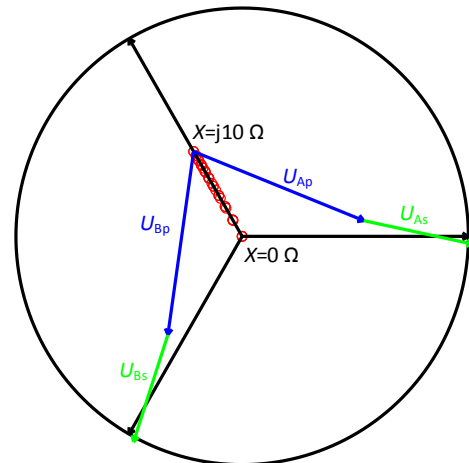


Fig. 10. Voltage potential of transformer neutral point in case of inductive grounding impedance

In some cases, neutral point can be grounded through inductive impedance to limit the fault current during the short-circuit conditions. Fig. 10 shows the voltages in parallel and series windings of healthy phases when inductive grounding impedance is equal to  $j10\ \Omega$ . Red circles show the path of neutral point voltage potential from solidly grounded neutral to  $j10\ \Omega$ , with resolution of  $j1\ \Omega$ . In case when transformer's neutral is grounded over reactance, voltages in series ( $U_{As}$ ,  $U_{Bs}$ ) and parallel windings ( $U_{Ap}$ ,  $U_{Bp}$ ) of healthy phases increase equally as shown in Fig. 10.

Single phase to ground faults are more common than previously analysed transformer terminal faults. Single phase to ground faults in phase C at HV side and at LV side are simulated considering different values of neutral grounding impedances. Fault locations are shown in Fig. 4. Table III shows calculated currents through autotransformer windings during different faults in phase C for case without stabilizing winding. Table IV shows the effect of stabilizing winding on current distribution along autotransformer windings.

TABLE III  
CURRENTS DURING FAULTS IN PHASE C WITH RESPECT TO NEUTRAL GROUNDING IMPEDANCE – WITHOUT STABILIZING WINDING

$I[A]/R[\Omega]$	Fault type	$R=0$	$R=10$	$R=100$	$R=\infty$
$I_{serA,B}$	*HV	1.2	123.1	663.9	785.6
	*LV	0.6	189.1	899.8	1017.9
	*TTF	1.2	959.1	1258.9	<b>1263.5</b>
$I_{serC}$	HV	2479.8	2461.8	1881.6	1579.6
	LV	<b>3852.7</b>	3803.9	2547.7	2042.1
	TTF	2479.8	1765.4	963.4	943.3
$I_{parA,B}$	HV	0.5	89.8	487.2	576.6
	LV	0.3	139.3	659.4	745.3
	TTF	0.5	701.7	920.9	<b>924.4</b>
$I_{parC}$	HV	1812.7	1799.6	1374.9	1153.5
	LV	<b>2816.8</b>	2780.7	1861.5	1491.3
	TTF	1812.7	1291.6	704.8	690.1

\*TTF – transformer terminal fault; HV, LV - single phase to ground faults at HV and LV side; bold marked - highest current values in each winding

TABLE IV  
CURRENTS DURING FAULTS IN PHASE C WITH RESPECT TO NEUTRAL GROUNDING IMPEDANCE – WITH STABILIZING WINDING

$I[A]/R[\Omega]$	Fault type	$R=0$	$R=10$	$R=100$	$R=\infty$
$I_{serA,B}$	*HV	44.9	56.9	96.9	98.6
	*LV	132.4	271.5	524.6	533.9
	*TTF	44.9	576.4	709	<b>710.8</b>
$I_{serC}$	HV	2530	2506	2374.8	2365.3
	LV	<b>3910.2</b>	3693.5	2773.7	2721.6
	TTF	2530	1483.1	186.1	36.2
$I_{parA,B}$	HV	185.3	288.1	585.8	601.1
	LV	558.4	615.5	785.9	793.4
	TTF	185.3	1750.4	2151.1	<b>2156.7</b>
$I_{parC}$	HV	1632.3	1575.8	1228.9	1202.1
	LV	<b>3515.9</b>	3207.1	1695.3	1586.7
	TTF	1632.3	1618.1	1610.3	1610.1
$I_{stab}$	HV	2755.6	3626.4	6542.1	6693.8
	LV	8323.1	7757.3	5256.6	5105.7
	TTF	2755.6	16916.8	20735	<b>20788</b>

Currents through stabilizing winding with respect to the neutral grounding impedance during different faults are shown in Fig. 11. The highest currents through the stabilizing winding for a directly grounded neutral point occurs in the case of single phase to ground fault in LV network. If neutral grounding

resistance exceeds  $3\ \Omega$ , currents through the stabilizing winding are highest in the case of transformer terminal fault.

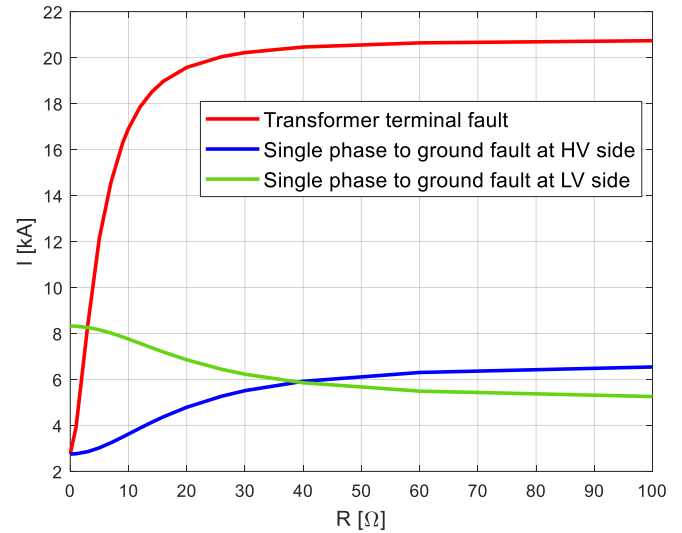


Fig. 11. Stabilizing winding currents during different faults with respect to the neutral grounding impedance

In previous analysis it was assumed that short-circuit impedance in the zero-sequence test is equal to the one in the positive-sequence test, which is valid for autotransformer with five-limb core and stabilizing winding. In this case, calculation results of inductance matrix model and BCTRAN model in EMTP showed good matching. Autotransformers may also be designed with three-limb core, to reduce cost, weight and losses. Simulations are performed in EMTP to investigate an effect of core type on short-circuit currents inside stabilizing winding. Zero-sequence in this case is approximately 80% of positive-sequence impedance ( $X_0 = 0.8 \cdot X_d$ ). Three-limb core did not show any significant effect on overvoltages in the network and at transformer windings, but it did affect currents in stabilizing winding. Fig. 12 shows an influence of core type on fault currents in stabilizing winding with respect to the neutral grounding impedance in the case of transformer terminal fault.

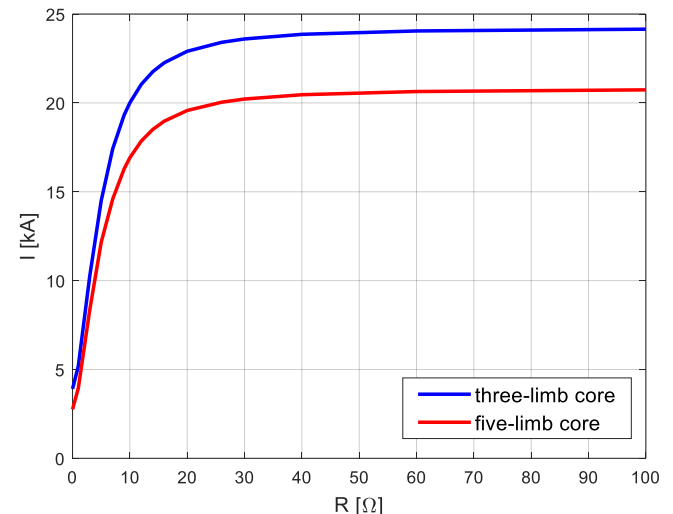


Fig. 12. Influence of core type on fault currents in stabilizing winding with respect to the neutral grounding impedance

The current through the stabilizing winding is approximately 20% higher in the case of a three-limb core compared to the five-limb core, which increases also thermal and mechanical stresses of the stabilization winding during a short-circuit.

## V. CONCLUSIONS

EMTP model of autotransformer with stabilizing winding is presented and compared with an inductance matrix model developed in Matlab. In the case of single-phase fault between transformer's HV terminal and neutral point, calculation results of both models showed good matching. The influence of stabilizing winding on temporary overvoltages and on fault current distribution among transformer's windings was analysed and the following conclusions can be drawn.

- Stabilizing winding affects the reduction of temporary overvoltages in healthy phases when transformer's neutral is isolated.
- Distribution of fault currents along autotransformer windings is highly influenced by presence of delta winding. Currents in faulty parallel windings increase while currents in faulty series windings reduce due to stabilizing winding.
- Stabilizing winding presence reduces the currents in healthy series windings and at the same time increases current in healthy parallel windings.
- If transformer's neutral is grounded over reactance, phase voltages in healthy phases increase equally. In the case of resistive grounding impedance, windings of one healthy phase experience higher voltage stress.
- Fault currents in stabilizing winding are higher in the case of autotransformer with three-limb core compared to the case with five-limb core.
- The highest currents through the stabilizing winding for a directly grounded neutral point occurs in the case of single phase to ground fault in LV network. If neutral grounding resistance increases, currents through the stabilizing winding are highest in the case of transformer terminal fault.
- Developed EMTP model can be applied to analyse how stabilizing (or tertiary) winding affects temporary overvoltages and fault current distribution along transformer windings. Model can be also applied for analysis of simultaneous faults on high-voltage and low-voltage side. Although these kinds of faults are relatively rare, they need to be analysed for correctly setting parameters of relay protection devices.

In the future work, FEM calculations on a transformer with known core geometry will be performed to obtain precise zero-sequence impedance and to incorporate it in inductance matrix model to get more accurate equivalent circuit of autotransformer based on the actual magnetic topology.

## VI. REFERENCES

- [1] J. J. Winders, Jr., "Power Transformers Principles and Applications", PPL Electric Utilities, Allentown, Pennsylvania, Marcel Dekker, 2002.
- [2] B. Filipovic-Grcic, I. Uglesic, A. Xemard, "Selection of station surge arresters for control of slow-front overvoltages on compact lines", Study Committee C4 on System Technical Performance, "A Colloquium on: Lightning and Power Systems - Technical Papers", Kuala Lumpur, Malaysia, pp. 1-14, 2010.
- [3] T. Kelemen, "Transformer Tertiary and How to Handle It", *Journal of Energy*, vol. 43, pp. 111-117, 1994.
- [4] Patricia Penabad-Duran, Xose M. Lopez-Fernandez, Casimiro Alvarez-Mariño, "Transformer Tertiary Stabilizing Windings. Part I: Apparent Power Rating", XX<sup>th</sup> International Conference on Electrical Machines (ICEM), 2012.
- [5] IEEE Std C57.12.00, "IEEE Standard for General Requirements for Liquid-Immersed Distribution, Power, and Regulating Transformers", The Institute of Electrical and Electronics Engineers Inc., 2015.
- [6] A. Ramos, J. Carlos Burgos, "Influence of tertiary stabilizing windings of three-phase three-legged YN<sub>yn</sub>d transformers on short-circuit performance of power grids", *Electric Power Systems Research*, vol. 144, pp. 89-95, March 2017.
- [7] J. G. Vlachogiannis, "An accurate autotransformer model for load flow studies effect on the steady-state analysis of the Hellenic transmission system", *Electric Power Systems Research*, vol. 50, pp. 147-153, May 1999.
- [8] R. G. Andrei, M. E. Rahman, C. Koepfel, and J. P. Arthaud, "A Novel Autotransformer Design Improving Power System Operation", *IEEE Trans. Power Delivery*, vol. 17, pp. 523-527, Apr. 2002.
- [9] B. A. Mork, F. Gonzalez, D. Ishchenko, "Leakage Inductance Model for Autotransformer Transient Simulation", presented at the International Conference on Power Systems Transients, Montreal, Canada, June 2005.
- [10] R. Horton, R. C. Dugan, K. Wallace, D. Hallmark, "Improved Autotransformer Model for Transient Recovery Voltage (TRV) Studies", *IEEE Trans. Power Delivery*, vol. 27, pp. 895-901, Apr. 2012.
- [11] D. Filipovic-Grcic, B. Filipovic-Grcic, K. Capuder, "Modeling of three-phase autotransformer for short-circuit studies", *International Journal of Electrical Power & Energy Systems*, vol. 56, pp. 228-234, 2014.
- [12] Z. Gajic, S. Holst, "Application of Unit Protection Schemes for Auto-Transformers", presented at the 2<sup>nd</sup> International Scientific and Technical Conference: Actual Trends in Development of Power System Protection and Automation, Moscow, September 2009.